PRODUCTION OF GAMMA-RAYS BY FAST NEUTRONS ON Fe AND Bi

V. M. Bondar, O. M. Gorbachenko, I. M. Kadenko, B. Yu. Leshchenko, Yu. M. Onishchuk, V. A. Plujko

Nuclear Physics Department, Taras Shevchenko National University, Kiev, Ukraine

Abstract

Time-of-flight method based on pulse neutron generator was applied for the measurements of prompt gamma-ray spectra of (n, xγ) reactions induced by fast neutrons on iron and bismuth. Experimental results are compared with theoretical calculations performed by the use of EMPIRE and TALYS codes. Sensitivity of the calculations to characteristics of excited nuclei was analyzed. Measured γ-ray spectra were used for the estimations of neutron capture cross sections.

1 Introduction

Nuclear data on neutron induced reactions are of special interest for the development of advanced reactor technologies as well as for studying of different nuclear reaction mechanisms, nuclear structure and decay processes. Gamma-emission is one of the most universal channels which accompanies any nuclear reaction. Therefore, in this contribution gamma-spectra of (n, xγ) reactions are investigated. We study reactions induced by 14.1 MeV neutrons on iron and bismuth which are also important for the development of fusion technologies.

Despite of numerous experimental measurements performed with ~14 MeV neutrons, data on γ-spectra in full energy range (up to excitation energy of the nucleus) are practically absent. In this contribution we present results of the γ-spectra measurements within the energy interval from 2 to 18 MeV. Differential cross sections of the (n, xγ) reactions for iron and bismuth were unfolded from amplitude instrumental spectra and cross section uncertainties were estimated. Measurement results are compared with theoretical calculations performed assuming gamma-emission from compound nucleus as well as emission on preequilibrium stages. Measured γ-ray spectra were used for the estimations of neutron capture cross sections.

2 Experimental measurements and data analysis

Measurements have been performed in circular geometry. Neutron pulse generator with $T(d,n)^4He$ reaction in Ti-T target was used as source of 14.1 MeV neutrons. Ring samples of iron and bismuth with mean radius 16 cm were placed on minimal distance from the neutron target. It provides optimal sample irradiation by source neutrons. The measurements of γ-spectra are performed using scintillation γ-spectrometer based on 15×10 cm NaI(Tl) detector. Prompt γ-rays were separated from source neutrons, background and rescattered γ-rays by the use of time-of-flight method combined with passive and active shielding. Flight path between the neutron source and detector was equal to 172 cm. The monitoring of neutron fluence was performed by the other plastic scintillator placed on 336 cm from neutron target at the angle 145 ° relatively to the deuteron beam line. More details concerning experiment can be found in Refs. [1-3].

Relation between amplitude spectra $U(V, \Delta V, \theta_\gamma)$ and differential cross section $\sigma_\gamma(E_\gamma, \theta) = d^2\sigma_\gamma(\theta_\gamma) / dE_\gamma d\Omega$ is given by the expression

$$U(V, \Delta V, \theta_\gamma) = \int_0^{E_{max}} dE_\gamma \cdot \sigma_\gamma(E_\gamma, \theta_\gamma) \int_{V-\Delta V/2}^{V+\Delta V/2} dV \cdot G\alpha(E_\gamma)\,\varepsilon(V, E_\gamma), \qquad (1)$$

where V is signal amplitude; ΔV - signal amplitude width; θ_γ - scattering angle; E_γ - γ-ray energy; G - geometry factor; $\alpha(E_\gamma)$ - energy-depended coefficient of the γ-ray self-absorption by sample detector; $\varepsilon(V, E_\gamma)$ - detector response function. Double differential cross section $\sigma_\gamma(E_\gamma, \theta_\gamma)$ have been measured at $\theta_\gamma = 90°$. Weak angle dependence of the cross section allows to estimate energy spectra $\sigma(E_\gamma)$ in the following way

$$\sigma(E_\gamma) \equiv \frac{d\sigma(E_\gamma)}{dE_\gamma} = 4\pi \cdot \sigma_\gamma(E_\gamma, \theta_\gamma). \qquad (2)$$

The expression for the detector response function $A(V, E_\gamma)$ was taken from Ref. [4]. It is based on analytical approximation of the bremsstrahlung experiment with correction on Monte Carlo simulations as well as on detection of 4.43 MeV γ-rays from neutron inelastic scattering on carbon.

According to the equations (1) and (2), the following Fredholm integral equation of the first kind should be solved to unfold cross section $\sigma(E_\gamma)$ from amplitude spectrum $U(V)$

$$\int_0^{E_{max}} A(V, E_\gamma)\sigma(E_\gamma)dE_\gamma = U(V), \quad A(V, E_\gamma) = \int_{V-\Delta V/2}^{V+\Delta V/2} dV \cdot G\alpha(E_\gamma)\,\varepsilon(V, E_\gamma), \qquad (3)$$

where $A(V, E_\gamma)$ - is total response function. There are problems in solving (3) due to instability of unfolded spectra to the experimental data uncertainties (so called ill-posed [5]). To find cross section $\sigma(E_\gamma)$ from inverse solving (3), an algorithm on the compact set of limited variations [4] was used. Uncertainties of the cross sections were estimated in assumption that the amplitude spectrum is distributed with Gauss distributions due to the large number of external factors. The uncertainties of the amplitude spectra were estimated as

$$\sigma_i = \sqrt{D_i + D_i^b}\ , \qquad (4)$$

where σ_i – standart deviation of the number of counts N_i ; i – number of channel; $D_i = N_i$ – variance of the number of counts N_i; $D_i^b = N_i^b$ – variance of the number of counts N_i^b corresponding to background measurements (without sample). Amplitude spectra were randomly varied with Gauss distribution and used for further unfolding of cross section values. Mean characteristics of the distribution were taken as equal to corresponding experimental values. Cross section uncertainties (standart deviations) were extimated by the use of uncertainties (4) as it was described in [3].

Experimental values of the unfolded differential cross sections and their uncertainties are shown on Fig. 2. As one can see, stable solution is obtained for the cross sections of ^{nat}Fe(n, xγ) and ^{nat}Bi(n, xγ) reactions using regularization algorithm on the compact set of limited variations. Set of monotonically decreasing functions were used for the unfolding of the cross sections. Rather good agreement of derived cross sections with experimental results from Ref. [6] is obtained.

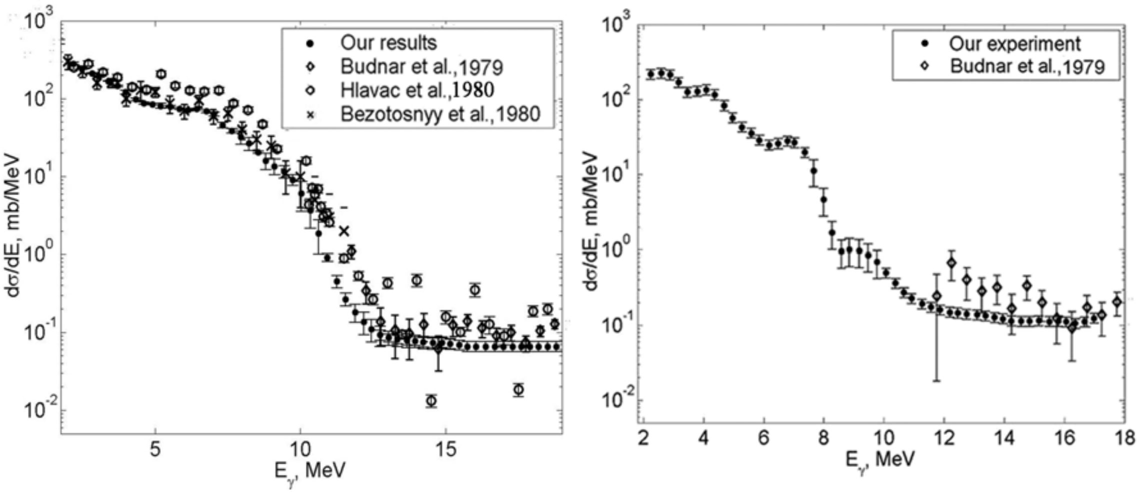

a *b*

Fig. 2. Differential cross sections of the reactions ^{nat}Fe(n, xγ) *(a)* and ^{nat}Bi(n, xγ) *(b)* derived using regularization algorithm on the compact set of limited variations: points – results of our experiment, rhombs – experimental data from [6], circles – [7], crosses – [8].

4 Results of the theoretical calculations

Experimental results were compared with theoretical calculations performed with taking into account both γ-emission from compound nucleus (CN) and preequilibrium emission [9]. Calculations of the γ-emission from CN were done using the Hauser-Feshbach statistical model. Within the framework of this model cross section of the reaction in the channel *b* is given by

$$\sigma_b(E,J,\pi)=\sigma_a(E,J,\pi)\frac{\Gamma_b(E,J,\pi)}{\Sigma_e\Gamma_e(E,J,\pi)},\qquad (5)$$

where σ_a – cross section of the compound nucleus production; *E* – excitation energy; *J* – spin; and π – parity of the CN state; Γ_b – width in the channel *b*; $\Sigma_e\Gamma_e$ – total width

$$\Gamma_e(E,J,\pi)=\frac{1}{2\pi\rho_{CN}(E,J,\pi)}\times\sum_{J'=0}^{\infty}\sum_{\pi'}\sum_{j=J'-J}^{J'+J}\int_0^{E-S_e}\rho_e(E',J',\pi')T_e^{l,j}(E-S_e-E')dE', \qquad (6)$$

S_e is the separation energy of the particle *e* from CN, ρ is nuclear level density and $T_e^{l,j}$ stands for the transmission coefficient for particle *e* with channel energy $\varepsilon=E-S_e-E'$ and orbital angular momentum *l* which together with particle spin *s* couples to the channel angular momentum j, J' and π' are spin and parity of the nucleus after reaction. In case of nucleons - transmission coefficient is calculated using optical model, whether for γ-rays - radiative strength function (RSF) [14] is used. As it can be seen from (5) and (6), the following input parameters are required for cross section calculations: optical potential, RSF and nuclear level density.

All the theoretical calculations presented below were performed for the isotopes of ^{56}Fe and ^{209}Bi whose abundances in natural elements which were used as samples in the measurements are 92% and 99% respectively.

Fig. 3 shows experimental differential cross sections of the reactions ^{nat}Fe(n, xγ) in comparison with theoretical calculations performed using EMPIRE [10] and TALYS [11] codes. In case of EMPIRE code the following input parameters were used in the calculations [14]: RSF within model of modified Loretzian (MLO) and Enhanced Generalized Super-Fluid Model (EGSM) for the nuclear level densities. In TALYS code RSF was calculated within Enchanced Generalized Loretzian (EGLO) with Gilbert-Cameron approach for nuclear level densities. These set of parameters are used in corresponding codes as default ones. Calculations have been performed with and without taking into account preequiliblirum emission within exiton model [9]. As an example we present results for the ^{nat}Fe(n, xγ) reaction cross sections. Similar results were also obtained for ^{nat}Bi(n, xγ) reactions.

As one can see from Fig. 3, rather satisfactory agreement of the theoretical calculations with experimental data is obtained for the ^{nat}Fe(n, xγ) reactions almost in all energy range accept intervals below 7 MeV and above 17 MeV, where calculated results exceed experimental ones. In order to get better agreement with experiment in the high energy range, preequilibrium processes should be corrected by factor 0.7. Calculations within EMPIRE and TALYS codes are in overall agreement.

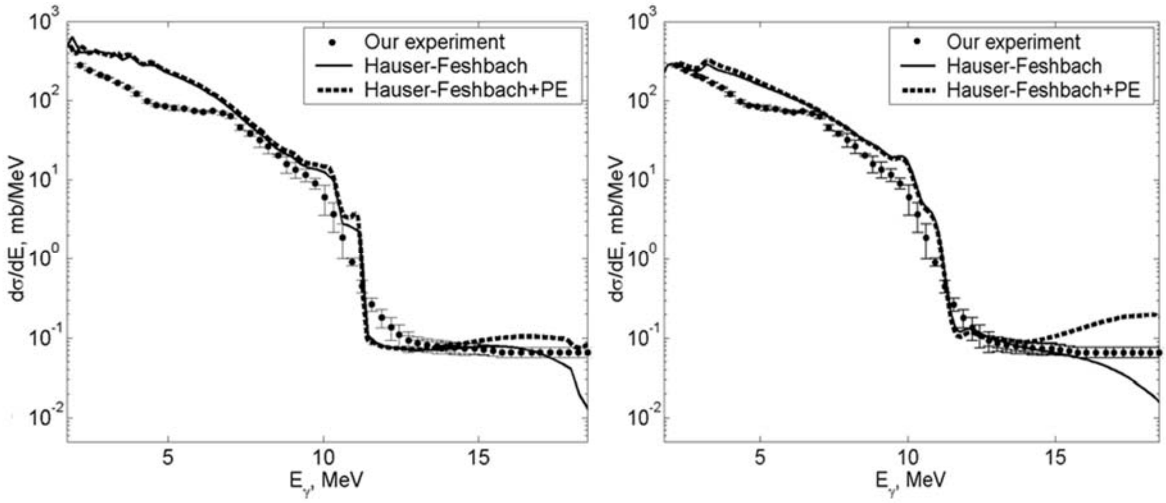

Fig. 3. Differential cross sections of the reactions ^{nat}Fe(n, xγ) performed using EMPIRE *(a)* and TALYS *(b)* codes: points – our experimental results, solid curve – calculations within Hauser - Feshbach statistical model, dashed curve – calculations within Hauser - Feshbach statistical model with taking into account preequilibrium emission (PE).

Sensitivity of the calculated cross sections to input parameters mentioned above was analyzed. Fig. 4 demonstrates the cross sections obtained by the use of different optical potentials taken from [12, 13]. EMPIRE code was used for the calculations. It can be seen from Fig. 4 that theoretical results obtained using both potentials gives rather satisfactory agreement with experimental results.

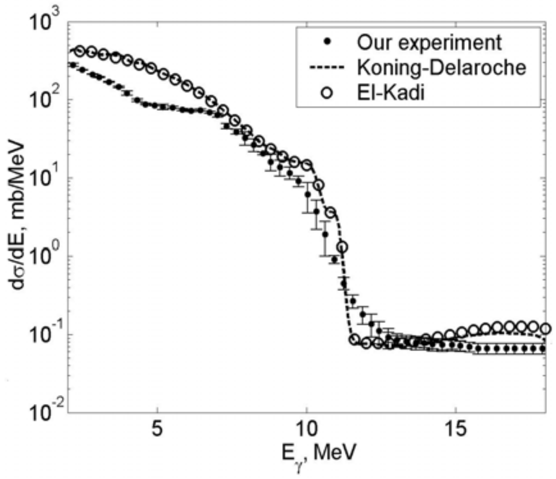

Fig. 4. Differential cross section of the reactions $^{nat}Fe(n, x\gamma)$ calculated with EMPIRE code using different optical potentials: points – our experimental results, dashed curve – Koning Delaroche potential [12], circles – El-Kadi potential [13],

It was checked that calculated cross sections are insensitive to the high values of the γ-ray transition multipolarity that is caused by the fact that number of the nuclear levels is large and electric dipole transitions are dominated.

To check sensitivity of the cross sections to the different models of electric dipole RSF, we performed calculations by the use the following approaches: Standart Loretzian (SLO), Enchanced Generalized Loretzian, different kinds of modified Loretzian, Generalized Fermi liquid (GFL) model. We also checked sensitivity of the calculations to the nuclear level densities. Enhanced Generalized Super-Fluid Model and Gilbert-Cameron approach are used in the calculations. Description of all the models mentioned above can be found in Ref. [14].

Fig. 5 demonstrates the example of the RSF and level density dependences of $^{nat}Fe(n, x\gamma)$ reaction cross sections.

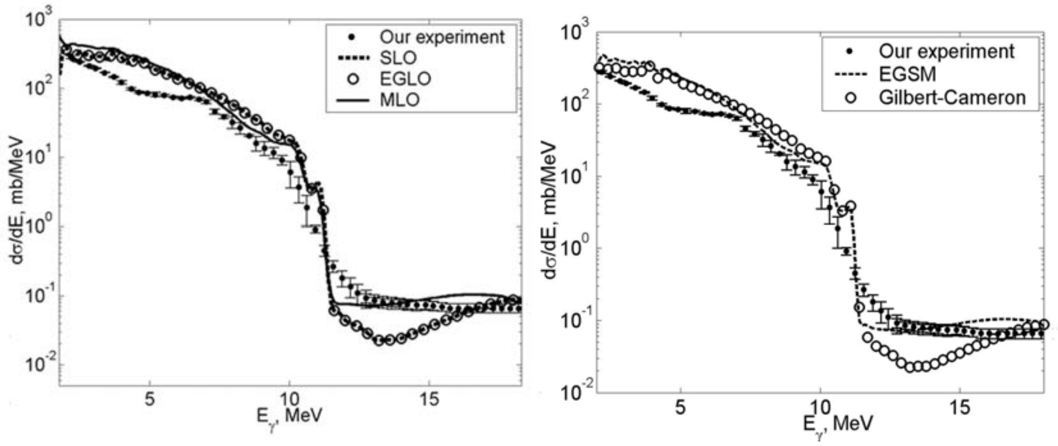

a *b*

Fig. 5. Differential cross sections of the $^{nat}Fe(n, x\gamma)$ reactions calculated with EMPIRE code using different models for the RSF *(a)*: dashed curve – SLO model, open circles – EGLO, solid line – MLO; and cross sections calculated by the use of different models for the nuclear

level densities within MLO model for RSF *(b)*: dashed curve – EGSM model, open circles – Gilbert – Cameron approach. Experimental results are shown by points.

As it can be seen, in the calculations performed by the use of EMPIRE code the best agreement with the experiment is obtained in case of using MLO model for RSF and EGSM model for the level densities.

From the results presented on Fig. 5, one can concludee that good agreement of the theoretical calculations with experimental results can be obtained in the case of simultaneous changes of the models both the radiative strength function and the nuclear level density. Similar results were obtained for ^{nat}Bi(n, xγ) reactions.

5 Estimation of the (n, γ) reaction cross sections

Prompt γ-ray spectra of (n, xγ) reactions measured by time-of-flight technique can be used for the estimations of neutron capture cross sections. It is of special importance since widely method of activation analysis is often inapplicable for measurements of (n, γ) reaction cross sections due to the effect of neutrons from output channel of (n, 2n) and (n, n′) reactions induced by the interaction of source neutrons with constructive materials of experimental setup. Capture process of these neutrons with low incident energies has extremely high cross section values and makes considerable contribution to the studied (n, γ) reaction cross-section increasing its value in few times. Measurements of prompt γ-rays with application of time-of-flight technique used in our research allows to avoid these problems.

In this contribution we used experimental prompt γ-ray spectra for the estimation of the ^{nat}Fe(n, γ) and ^{nat}Bi(n, γ) reaction cross sections. There are only two experimental data sets on these cross sections in EXFOR database (http://www-nds.iaea.org/exfor/).

After the interaction of neutron with incident energy E_n with atomic nucleus, excitation energy of the compound nucleus is equal to $U_{nC} = E_n + S_n$, where S_n is neutron separation energy. It can be assumed that experimental γ-spectra within the energy interval from E_n up to excitation energy U_{nC} correspond to γ-rays produced in (n, γ) reactions since in this region probability of particle emission is low. Therefore, (n, γ) reaction cross sections can be estimated by the integrating of the γ-ray spectra in the energy range from E_n up to excitation energy of the nucleus U_{nC}. Namely, in this work integration of γ-spectra was performed from approximately 14 MeV up to U_{nC} =21.5 MeV in case of ^{nat}Fe(n, γ) reaction and U_{nC} =18.6 MeV for ^{nat}Bi(n, γ) reaction. Such a method of cross section estimations for ^{nat}Fe(n, γ) and ^{nat}Bi(n, γ) reactions were firstly used in the work [6].

Fig. 6 shows cross sections of ^{nat}Fe(n, γ) and ^{nat}Bi(n, γ) reactions estimated in our experiment and compared with theoretical calculations and results from Refs. [6, 15, 16]. Theoretical calculations of the cross sections have been performed within Hauser-Feshbach statistical model combined with exiton preequilibrium model. Code TALYS with default set of parameters was used for the calculations.

As one can see from Fig.6, in case of ^{nat}Fe(n, γ) reaction our experimental results are in agreement with theoretical predictions and exceed results from Ref.[6] on approximately 30%. For ^{nat}Bi(n, γ) reaction our results agree with theoretical calculations and results from Refs.[15, 16]. It should be noted that experimental γ-spectra also include γ-rays from (n, γ) reactions with energies below E_n, which we can't take into account since other (n, xγ) reactions are dominated in this energy range. However, contribution of γ-rays from (n, γ) reaction with energies below E_n is low. Therefore, experimental results are in good agreement with theoretical predictions.

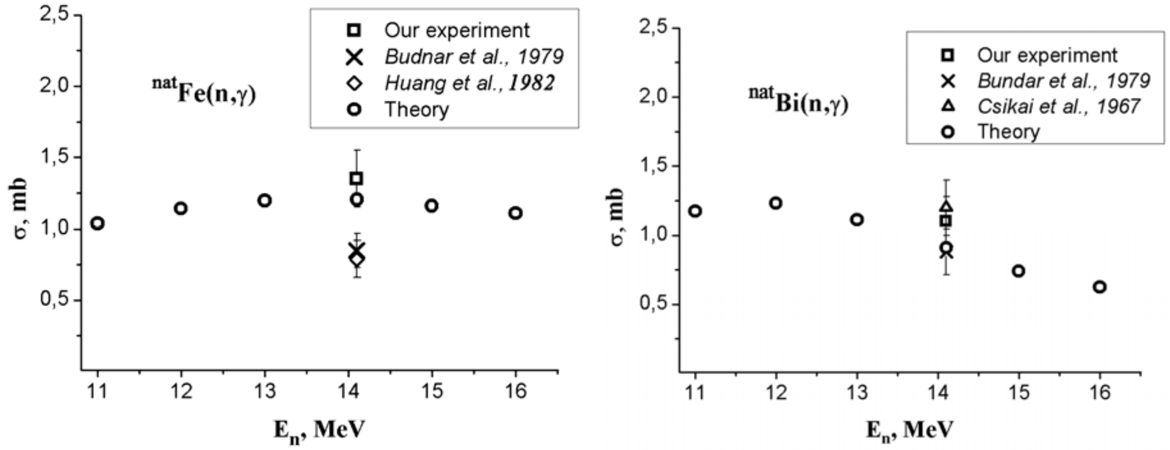

Fig.6. Cross section estimations for ^{nat}Fe(n, γ) *(a)* and ^{nat}Bi(n, γ) *(b)* reactions: squares – results of our experiment, open circles – theoretical calculations, crosses - experimental data from [6], rhombs – [15], triangles – [16].

Conclusions

Differential cross sections of ^{nat}Fe(n, xγ) and ^{nat}Bi(n, xγ) reactions were measured using time-of-flight technique. The algorithm on the compact set of limited variations was used in order to obtain the cross sections values.

Theoretical calculations of the cross sections are performed considering gamma-emission both from equilibrium and preequilibrium stages. Results of the calculations within EMPIRE and TALYS codes are rather overall agreement and general behaviour of the theoretical results is in agreement with experimental ones.

In order to obtain the best agreement of calculated cross sections with experimental results, the optimal set of input parameters should be used, namely models for RSF, nuclear level densities and optical potential. According to our analysis, cross sections of ^{nat}Fe(n, xγ) and ^{nat}Bi(n, xγ) reactions calculated by the use of EMPIRE code within MLO RSF model with EGSM model for the nuclear level densities give the best agreement with experimental results.

Prompt γ-ray spectra were used for the estimations of ^{nat}Fe(n, γ) and ^{nat}Bi(n, γ) reaction cross sections. Obtained results are in agreement with theoretical predictions performed by the used of TALYS code. In case of ^{nat}Bi(n, γ) reaction our results also agree with results from Ref.[6]. For the ^{nat}Fe(n, γ) reaction our cross section values exceed results from Refs.[15, 16] on approximately 30%.

.

Acknowledgments. V.M. Bondar expresses her deep gratitude to the Organizing Committee of the Conference for financial support and warm welcome.

REFERENCES

1. V. M. Bondar, I. M. Kadenko, B. Yu. Leshchenko et al., Nucl. Phys. At. Ener. **1(23)** (2008) 16 (in Ukrainian).
2. V. M. Bondar, I. M. Kadenko, B. Yu. Leshchenko et al., Bull. Russian Acad. Sciences: Physics. **73(11**) (2009) 1511.
3. V. M. Bondar, I. M. Kadenko, B. Yu. Leshchenko et al., *Reactor Dosimetry State Of The Art 2008: Proc. 13th Int. Symp.* (25-30 May, 2008, Alkmaar, Netherlands), World Scientific Publ. Co., Singapore. (2009) 516.
4. G. M. Gurevich, V. M. Mazur, G. V. Solodukhov, Instr. Exp. Techn. **2** (1975) 59.
5. A. N. Tikhonov, A. V. Goncharsky, V. V. Stepanov et al., Numerical methods for the solution of ill-posed problems, Nauka, Moscow, 1990 (in Russian).
6. M. Budnar, F. Clevba, E. Hodgson et al*.*, Nucl. Instr. Meth. **44** (1966) 292; R,INDC(YUG) - ***6*** (1979).
7. S. Hlavac, P. Oblozinsky*, Neutron Induced Reactions: Proceedings of the 2^{d} Int. Symp.: Physics and applications* (25-29 June, 1979, Smolenice), VEDA Pub. House of the Slovak Acad. of Science, Bratislava.**Vol. 6** (1980) 395.
8. V. M. Bezotosnyi, V. M. Gorbachev, M. A. Efimova et al., Atomic Energy. **4** (1980) 239.
9. E. Gadioli, P.E. Hodson. Pre-Equilibrum Nuclear Reactions, Clarendon Press, Oxford, 1992.
10. M. Herman, R.Capote, B.V. Carlson et al., Nucl.Data Sheets. **108** (2007) 2655.
11. A. J. Koning, S . Hilaire, M. C. Duijvestijn, In *Proc. of the International Conference on Nuclear Data for Science and Technology*, ND2007 (April 22 – 27, 2007, Nice, France), 2008 CEA, published by EDC Sciences, Vol. **1** (2008) 211.
12. A.J. Koning, J.P. Delaroche, Nucl. Phys. **A713** (2003) 231.
13. S. M. El-Kadi, C. E. Nelson, F. O. Purser et al., Nucl. Phys. **A390** (1982) 509.
    R. Capote, M. Herman, P. Oblovzinsky et al., Nucl. Data Sheets. **110** (2009) 3107; http://www-nds.iaea.org/RIPL-3/.
14. Zheng-De Huang,Cao Zhong, Wang Hui-Zhu et al., *Proceedings of 4th Symp. Neutr. Capt. Gamma-Ray Spectrosc.* (Grenoble 1981), Inst. Phys. Publishing Inc. (1982) 512.
15. J. Csikai, G. Peto, M. Buczko et al., Magyar Fizikai Folyoirat. **16** (1967) 123.